JOURNAL OF THERMOPHYSICS AND HEAT TRANSFER
Vol. 23, No. 2, April–June 2009

Heat Transfer in Trailing-Edge Channels with Slot Ejection Under High Rotation Numbers

Yao-Hsien Liu* and Michael Huh†
Texas A&M University, College Station, Texas 77843-3123
Lesley M. Wright‡
Baylor University, Waco, Texas 76798-7356
and
Je-Chin Han§
Texas A&M University, College Station, Texas 77843-3123

DOI: 10.2514/1.37982

The regionally averaged heat transfer coefficients were measured in a wedge-shaped channel ($D_h = 2.22$ cm, $A_c = 7.62$ cm^2) to model an internal cooling passage near the trailing edge of a gas turbine blade. This test section was configured so that the inlet coolant exhausts through the slots to simulate the trailing-edge ejection. Therefore, the local mass flow rate decreases along the streamwise direction due to the coolant discharging through the slots. The effects of slot ejection enhance heat transfer near the narrow side while decreasing heat transfer on the wide side of the channel at the stationary condition. The inlet Reynolds number of the coolant varies from 10,000 to 40,000, and the rotational speeds vary from 0 to 500 rpm. The inlet rotation number varies from 0 to 1.0. The local rotation number and buoyancy parameter vary by the different rotational speeds and local Reynolds number in each region. Detailed spanwise and streamwise heat transfer distributions are strongly affected by the slot ejection at both the stationary and rotating conditions. This study shows that the rotation number and buoyancy parameter are useful parameters to correlate the effect of rotation on heat transfer in the current study.

Nomenclature

A	=	projected surface area of a copper plate segment
A_j	=	cross-sectional area of the slot
AR	=	channel aspect ratio, $W{:}H$
Bo_x	=	local buoyancy parameter, $(\Delta\rho/\rho)_x Ro^2 (R_x/D_h)$
C_D	=	discharge coefficient
D_h	=	channel hydraulic diameter
H	=	channel height
h	=	regionally averaged heat transfer coefficient
k	=	thermal conductivity of the coolant
L	=	length of the heated portion of the test section
$\dot{m}_j$	=	mass flow rate through the jth slot
$\dot{m}_n$	=	mass flow rate radially at the exit of the nth region
$\dot{m}_{xn}$	=	local mass flow rate at the nth region
Nu	=	regionally averaged Nusselt number
Nu_o	=	Nusselt number for fully developed turbulent flow in a nonrotating smooth pipe
Nu_s	=	regionally averaged Nusselt number under stationary condition
P_{exit}	=	pressure at the exit of the slot
P_{in}	=	pressure at the inlet of the slot
Pr	=	Prandtl number of the coolant
Q_{loss}	=	external heat loss
Q_{net}	=	net heat transfer
R	=	mean radius of rotation (from the center of rotation to center of heated channel)
R_x	=	local radius of rotation (from the center of rotation to local region within heated channel)
Re_x	=	local Reynolds number
Re_i	=	Reynolds number at the inlet of the test section
Ro	=	rotation number, $\Omega D_h/V$
Ro_i	=	inlet rotation number, $\Omega D_h/V_i$
Ro_x	=	local rotation number, $\Omega D_h/V_x$
$T_{b,x}$	=	local coolant bulk temperature
$T_{f,x}$	=	local film temperature
$T_{w,x}$	=	regionally averaged wall temperature
V	=	bulk velocity of the coolant in the streamwise direction
V_i	=	bulk velocity of the coolant at the inlet of the test section
W	=	channel width
$(\Delta\rho/\rho)_{\text{in}}$	=	inlet coolant-to-wall density ratio, $(T_w - T_{bi})/T_w$
$(\Delta\rho/\rho)_x$	=	local coolant-to-wall density ratio
β	=	angle of channel orientation with respect to the axis of rotation
μ	=	viscosity of the coolant
ρ	=	density of the coolant
Ω	=	rotational speed

Received 9 April 2008; revision received 5 January 2009; accepted for publication 19 January 2009.

*Research Assistant, Department of Mechanical Engineering.
†Research Assistant, Department of Mechanical Engineering.
‡Assistant Professor, Department of Mechanical Engineering. Member AIAA.
§Distinguished Professor and M.C. Easterling Chair Professor, Turbine Heat Transfer Laboratory, Department of Mechanical Engineering; jc-han@tamu.edu. Associate Fellow AIAA.

Introduction

ADVANCED gas turbines operate at high temperatures to improve thermal efficiency. To protect the turbine blade from damage due to high temperatures, external (film) and internal cooling are applied to the turbine blades. Internal cooling is achieved by circulating compressed air in the multipass flow channels inside the blade structure. As shown in Fig. 1, the cross section of the internal cooling channels varies depending on their location in the blade. Cooling channels near the leading edge could be tall and narrow, whereas channels closer to the trailing edge are typically wide and short. The cooling channels are either single pass (with radial outward flow) or multipass (both radial outward and radial inward

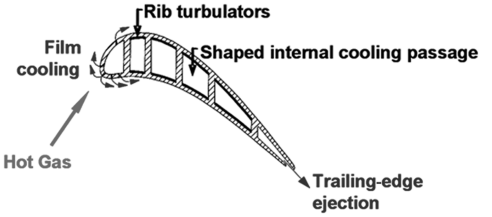

Fig. 1 Typical internal cooling passages of a cooled gas turbine blade.

flow). Ribs or other turbulence promoters are typically applied to enhance heat transfer inside the blade passage.

Many studies on advanced gas turbine cooling technology are reviewed in [1]. It is necessary to understand the behavior of the coolant through smooth, nonrotating channels before more complicated behavior can be fully realized. Turbulent flow through nonrotating, circular tubes has been thoroughly investigated by Kays and Crawford [2]. They summarized the heat transfer in tubes with various entrance conditions. The Nusselt number in tubes with fully developed turbulent flow is also given by Kays and Crawford [2]. The widely accepted Dittus–Boelter–McAdams correlation for fully developed turbulent flow was developed in circular tubes, but this correlation has also been applied to the flow through channels with noncircular cross sections.

However, the actual turbine blade is rotating. The studies in the nonrotating channel have been extended to the rotating channel by several groups. Wagner et al. [3,4] show the heat transfer from the leading and trailing walls of a rotating channel are not symmetrical. In other words, in their square ($AR = 1{:}1$) cooling channel with radially outward flow, the heat transfer from the trailing surface increases with rotation, whereas the heat transfer from the leading surface decreases. Johnson et al. [5] extended this study of a square channel to investigate the effect of channel orientation with respect to the direction of rotation. When the channel is oriented nonorthogonally to the direction of rotation, the effect of rotation decreases; in other words, the difference between the heat transfer coefficients on the leading and trailing surfaces is reduced. Dutta and Han [6] confirmed this result in a rotating, square channel.

When the impact of rotation was realized, researchers sought more detailed heat transfer measurements. Park and Lau [7] used naphthalene sublimation to obtain detailed heat/mass transfer distributions in a rotating, two-pass, square channel. The detailed distributions indicated that the Coriolis forces create large spanwise variations on both the leading and trailing surfaces. Bons and Kerrebrock [8] gathered detailed heat transfer coefficient distributions using infrared thermography, and they completed these heat transfer measurements with flowfield measurements (particle image velocimetry). In this rotating, single-pass, square channel, they concluded that the reduced heat transfer from the leading wall is the result of the Coriolis force transporting the hot, low-momentum wall fluid from the trailing wall to the leading wall.

Cooling channels with different aspect ratios have been applied to different locations of the turbine blade, and the aspect ratio effect should be considered. Azad et al. [9] studied the combined effect of channel aspect ratio and channel orientation. Their findings for a 2:1 (width : height), two-pass channel were similar to a 1:1 channel: in the first pass with radially outward flow, the heat transfer from the leading surface decreased whereas the trailing surface increased, and the opposite occured in the second-pass. Also, the effect of rotation is reduced when the channel is skewed to the direction of rotation.

Channels located near the trailing edge of the blade have an even greater aspect ratio to fit into this narrow region of the blade. Several studies have focused on the effect of rotation in a 4:1 channel. Griffith et al. [10] observed significant spanwise variation in the heat transfer distributions due to rotation. Their results also showed that the channel orientation of the 4:1 channel has a small effect on the trailing surface and a large effect on the leading surface in this one-pass cooling channel. In the 4:1 channel oriented at 135 deg to the direction of rotation, the heat transfer from all surfaces in the channel is enhanced with rotation. Wright et al. [11] studied the effect of entrance geometry on the heat transfer enhancement in the rotating rectangular channel (4:1). They showed that, with the simultaneous development of both the hydrodynamic and thermal boundary layers, the Nusselt number ratios may not reach the fully developed values predicted by the Dittus–Boelter–McAdams correlation. Acharya et al. [12] used the mass transfer technique to obtain detailed distribution in a two-pass 4:1 channel, and their findings were consistent with Griffith et al. [10]. Zhou et al. [13] considered the effect of rotation in a 4:1 channel with high rotation numbers. They concluded that there is a critical rotation number beyond which the expected heat transfer trends reverse. They also showed that increasing the density ratio increases the heat transfer enhancement. Fu et al. [14,15] showed how the heat transfer enhancement varied in smooth channels with five different aspect ratios depending on the channel cross section, rotation number, and buoyancy parameter.

The channels near the leading edge may have a triangular cross section, whereas the channels near the trailing edge may also be triangular or trapezoidal. The heat transfer and friction coefficients measured in smooth equilateral triangles are in good agreement with the established correlations developed for the tube flow, with the hydraulic diameter of the triangular duct replacing the tube diameter [16,17]. When the cross section of the channel changes from an equilateral triangle to a scalene triangle, similar conclusions are drawn. Obot [18] concluded that the heat transfer coefficients measured in the fully developed region of a scalene triangular duct are comparable to those predicted by the established Colburn equation for fully developed, turbulent flow through a smooth tube. Similar conclusions were drawn by Zhang et al. [19] with their right-triangle duct; in their channel with smooth walls, the heat transfer coefficients were adequately predicted with the Dittus–Boelter–McAdams correlation whereas the friction factors could be established with the Blasius equation for turbulent flow through smooth tubes.

The effect of rotation on heat transfer has also been measured in triangular channels. Harasgama and Morris [20] concluded that the effect of rotation in a triangular duct with radially outward flow can be estimated by correlations developed for circular tubes. Dutta et al. [21] showed that, in the first pass of a triangular channel with radially outward flow, the heat transfer coefficients on the trailing and side walls are enhanced with rotation, whereas the heat transfer coefficients on the leading surface decline.

The coolant in the trailing-edge cooling passages is likely to be extracted for trailing-edge ejection, either through discrete holes or slots, to further protect the trailing edge of the blade. Kumaran et al. [22] studied heat transfer in a rectangular pin fin channel with short and long ejection holes. They found that the heat transfer in the pin fin channel with sidewall ejection flow is about 25–30% lower than that with the straight flow. Taslim et al. [23] used a more realistic trapezoidal (wedge-shaped) channel with trailing-edge ejection. They showed that, in a smooth, wedge-shaped channel, the average heat transfer coefficients were adequately predicted with the Dittus–Boelter correlation. They also showed that significant spanwise variation is present in this channel. However, when trailing-edge ejection is introduced, this spanwise variation is reduced due to the lateral flow. Hwang and Lu [24] also studied the effect of trailing-edge ejection in trapezoidal ducts. They confirmed that the fully developed heat transfer coefficients in the trapezoidal duct (without bleed flow) are comparable to those predicted by the Dittus–Boelter correlation. They also concluded that an increase in the ejection rate increases the heat transfer coefficients on the narrow side of the channel at the cost of reducing the heat transfer coefficients on the wide side of the channel.

Based on the data available in the open literature, the objective of the current study is as follows: 1) to study the effect of rotation in trailing-edge cooling channels with slot ejection, especially under high rotation numbers close to the real engine condition; 2) to determine how the slot ejection affects the heat transfer enhancement in the streamwise and spanwise directions; 3) to determine the variation of the coolant flow remaining in the channel after the coolant flow is discharged through the slots to investigate the effects

on heat transfer enhancement and the effect of rotation; and 4) to reexamine the validity of the rotation number and buoyancy parameter, two nondimensional parameters which have already been proved to be able to quantify the effect of rotation in the smooth channels [25,26].

Experimental Facility

Rotating Facility

With the blades rotating in the engine, the rotation number associated with the coolant is in the range of 0.2–0.3. One method of obtaining the desired range of rotation numbers with the applicable Reynolds numbers is to run the laboratory experiments at an increased pressure. With the coolant pressurized above atmospheric pressure, at a given mass flow rate (Reynolds number), the density increases while the coolant velocity decreases. The decreased velocity yields increased rotation numbers.

As shown in Fig. 2, coolant is supplied to the rotating rig via a two-pass rotary union located at the base of the rig. Upstream of the rotary union, the inlet coolant mass flow rate is measured with a square-edge American Society of Mechanical Engineers orifice meter. The coolant travels upward through an insulated hose placed inside a hollow shaft. The air is then ducted through the support head of the rotating arm, and an insulated hose transports the air to the test section contained within a pressure vessel located at the end of the rotating arm. The coolant passes through the test section, and the air travels through a second hose as it leaves the pressure vessel. The air travels through the support head and downward through the hollow shaft (annularly outside the hose used to supply the coolant). The return air then passes through the rotary union, and a ball valve is used to maintain the desired backpressure.

As in the previous studies, a motor is used to drive the rotating arm. The motor is connected to a variable frequency drive, so that the rotational speed of the arm can be varied. For the present study, the rotational speed varies from 0 to 500 rpm. A 100-channel slip ring is located above the rotating arm to transfer thermocouple signals, pressure transducer signals, and resistance heater electricity to the rotating arm. Mounted above the slip ring is a 48-channel Scanivalve pressure transducer.

Trailing-Edge Test Section

Figure 3a shows the design of the present test section. This new geometry is more appropriate to fit the blade profile near the trailing edge of the turbine blade. The cross section of the channel is a wedge (or trapezoid). The side wall (close to the middle portion of the blade) is 2.54 cm tall, and the cross section narrows to 0.32 cm near the trailing edge of the blade. The distance from the innermost side to the outermost side is 5.28 cm. If the channel were extended to form an isosceles triangle, the apex angle of the triangle would be 23.5 deg. Six slots were machined at the narrow side of the wedge-shape section as shown in Fig. 3b. The width and the length of each slot are 0.16 cm and 1.27 cm, respectively. The distance between each slot is 1.27 cm. The heated length of the channel is 15.56 cm, as shown in Fig. 3c, and, with a hydraulic diameter of 2.25 cm, this gives an overall heated length-to-hydraulic diameter ratio (L/D_h) of 6.30. The distance from the center of rotation to the center of the heated channel is 67.8 cm. The air enters an unheated entrance with a rectangular cross section of 5.38 cm wide by 3.18 cm tall. Two mesh screens are positioned in this entrance region to help spread the flow before it reaches the heated portion of the test section. With this

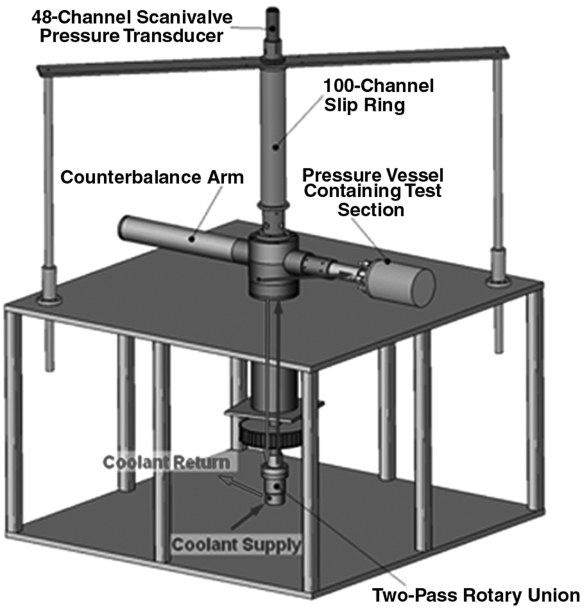

Fig. 2 Rotating facility for the internal turbine blade heat transfer studies.

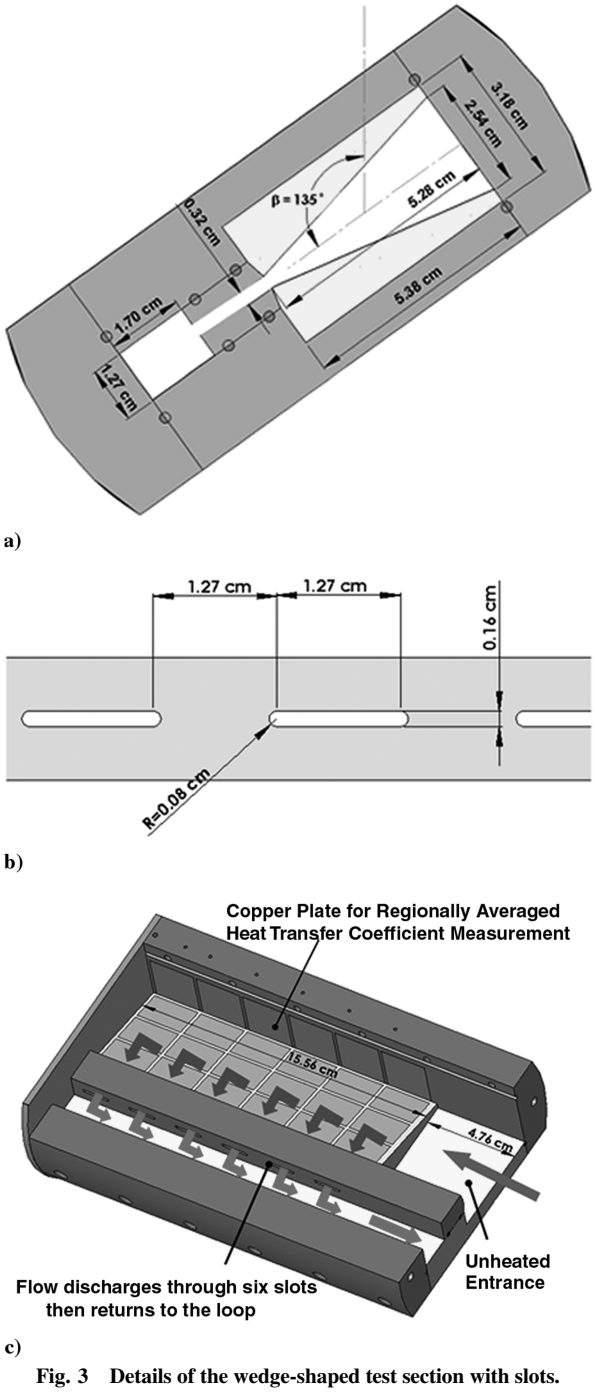

Fig. 3 Details of the wedge-shaped test section with slots.

entrance configuration, the air is forced through a sudden contraction before it enters the heated test section. Obviously, with the wedge-shaped cross section, the contraction ratio is much greater near the outer wall (9.9:1) of the test section than the inner wall (1.25:1). The length of the entrance region is 4.76 cm.

Although only the first pass, with radially outward flow, of the test section is instrumented for heat transfer measurements; a second pass is needed to return the flow and maintain the desired pressure within the test section. The first pass of the channel is dead-ended; thus, all the flow discharges through these six slots into the second pass. This second pass for returning the flow has a rectangular cross section of 1.70 cm wide by 1.27 cm high. The flow ejected from the six slots then travels through the second pass back to the flow loop.

To measure the heat transfer variation across the width (or span) of the channel, both the leading and trailing surfaces are divided into three regions each. Figure 4 shows how these six regions, combined with the inner side wall, give a total of seven regionally averaged heat transfer coefficient measurements. Each region consists of a single copper plate with a 0.318 cm thickness. Each copper plate has a 0.159 cm blind hole in the backside, with a thermocouple mounted in the hole with high conductivity thermal epoxy. Six regions are used in the streamwise (flow) direction, and so a total of 42 regions comprise the test section. The outermost wall (near the trailing edge) is left uninstrumented for the slot ejection in the current study.

Electric resistance heaters are fixed beneath the copper plates. One heater services six copper plates; each spanwise region has an individual heater. In other words, one heater is used to heat all six copper plates of the side wall, and one heater is used for the six plates of the trailing inner surface, and so on. The wall temperature of 65°C is maintained at the middle location ($x/Dh = 4.0$) of the test section, and the wall temperature range is within 45–65°C. High-conductivity thermal paste is applied to each heater to minimize the contact resistance between the heater and the copper plates. The copper plates are mounted in the test section support structure, which is fabricated from canvas electrical grade garolite. The insulating material reduces the heat loss from the heaters to the support material. The test section is assembled and placed in the pressure vessel. Additional insulating material is used to fill the air gaps between the test section and the wall of the pressure vessel.

Pressure taps are instrumented at the inlet and exit of the slots and are connected to a 48-channel Scanivalve pressure transducer. The pressure transducer then transfers the signals obtained through the slip ring to the data acquisition system. The coolant air enters the test section at 6 times the atmospheric pressure (608 kPa, abs), with the pressure ranging from 608–600 kPa inside the entire channel; this pressure is maintained for all cases, both stationary and rotating. The Reynolds number at the inlet is controlled at 10,000, 20,000, 30,000, and 40,000. The channel is orientated 135 deg to the direction of rotation (similar to the trailing-edge passage as shown in Fig. 1). The rotational speed of the channel is varied from 0 to 500 rpm. The inlet rotation number varies from 0 to 1.0.

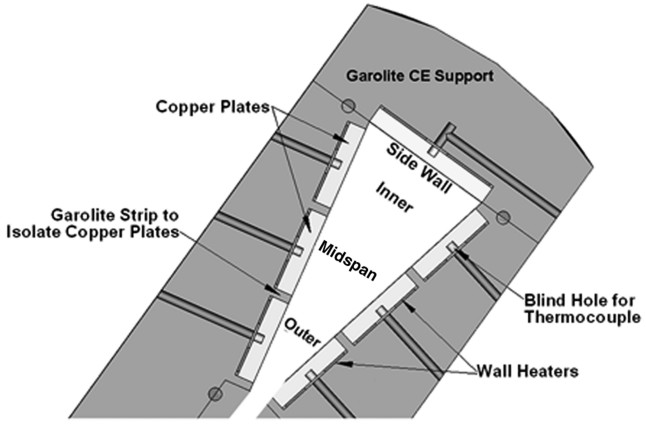

Fig. 4 Schematics of the test section.

Data Reduction

As described in the experimental setup, regionally averaged heat transfer coefficients are measured in the current study. The regionally averaged heat transfer coefficients can be determined from Newton's Law of Cooling as follows:

$$h = \frac{\dot{Q}_{\text{net}}}{A(T_{w,x} - T_{b,x})} = \frac{\dot{Q}_{\text{in}} - \dot{Q}_{\text{loss}}}{A(T_{w,x} - T_{b,x})} \tag{1}$$

The net rate of heat transfer is determined from the difference of the power supplied to each resistance heater and the heat lost from the test section. The heat losses are determined from a calibration where the insulation is inserted into the channel. Power is supplied by the heaters, and the power required to reach a series of given temperatures is recorded. With the insulating material placed inside the channel, the power supplied to the heaters during this calibration is equivalent to the heat lost during the actual cooling trials. Separate heat loss calibrations are required for each rotational speed. At the lowest inlet Reynolds number of 10,000, heat losses account for approximately 21% of the power supplied to each heater in the stationary channel and 23% in the channel rotating at 500 rpm. However, when the inlet Reynolds number increases to the maximum value of 40,000, the heat losses range from 8% in the stationary channel to 10% in the rotating channel (500 rpm).

The regional wall temperature ($T_{w,x}$) is measured using the thermocouple fixed in each copper plate. The coolant bulk temperature at a specific location ($T_{b,x}$) in the channel is determined based on the measured inlet and outlet temperatures. With thermocouples placed in the flow in the inlet section and exit of the last slot, the inlet and outlet bulk temperatures are known. Therefore, the temperature of the coolant at any location within the channel can be calculated using linear interpolation.

The measured heat transfer coefficients can be represented by the nondimensional Nusselt number. Although the Nusselt number is useful to extend the results from the laboratory to the actual engine, it is often more useful to normalize the Nusselt number to quantify the heat transfer enhancement (or declination) due to either the specific channel geometry or rotation. The Nusselt number ratio (Nu/Nu_o) is used to show the heat transfer enhancement relative to fully developed, turbulent heat transfer in a circular tube. This fully developed, turbulent heat transfer can be expressed with the Dittus–Boelter–McAdams correlation for heating:

$$\frac{Nu}{Nu_o} = \left(\frac{hD_h}{k}\right)\left(\frac{1}{0.023Re^{0.8}Pr^{0.4}}\right) \tag{2}$$

However, the local mass flow rate decreases along the streamwise direction due to slot ejection, and the coolant flow remaining in the channel needs to be determined to obtain the accurate Nu_o. The estimated mass flow rate through the jth slot can be calculated by Eq. (3) from Kumaran et al. [22]:

$$\dot{m}_j = C_D A_j [2\rho(P_{\text{in}} - P_{\text{exit}})]^{1/2} \tag{3}$$

where C_D is the discharge coefficient, and A_j is the cross-sectional area of the slot. The density is obtained by the pressure and bulk temperature at each location. The pressure is measured by the pressure taps at the inlet and exit of the slot. The bulk temperature is obtained by the linear interpolation of the inlet temperature and outlet temperature of the channel. The sum of the mass flow rate through these six slots is equal to the total mass flow rate at the inlet of the channel. The same discharge coefficients through these six slots were assumed and the ratio of the mass flow rate radially into the nth region to the inlet mass flow of the channel can be determined as follows:

$$\frac{\dot{m}_n}{\dot{m}} = 1 - \frac{\sum_{n=1}^{n-1} \dot{m}_j}{\dot{m}} \tag{4}$$

where $\sum \dot{m}_j$ is the sum of the mass flow rate through the slots upstream of the nth region at which the value of $\dot{m}_n$ is to be

calculated, and $\dot{m}$ is the mass flow rate at the inlet. There are a total of six regions in the streamwise direction within the channel. The local mass flow rate in each region (at x) of the channel is the average of the radially inlet and radially outlet mass flow in that region:

$$\frac{\dot{m}_{xn}}{\dot{m}} = \frac{\dot{m}_{n-1} + \dot{m}_n}{2\dot{m}} \tag{5}$$

The experimental uncertainty for the presented results was calculated using the method developed and published by Kline and McClintock [27]. At the inlet Reynolds number of 10,000, at which the most uncertainty exists in the measured quantities, the overall uncertainty in the Nusselt number ratio is approximately 16.9% of the presented values. However, at the higher Reynolds numbers, the percent uncertainty of the individual measurements decreases, and the overall uncertainty in the Nusselt number ratio decreases to approximately 5.8% of the calculated value at the highest inlet Reynolds number of 40,000.

Results and Discussion

The heat transfer in both the stationary and rotating trailing-edge cooling channels is considered. The stationary channel provides baseline results before considering the effect of rotation. The results reported are based on the seven regions as shown in Fig. 4. These regions are the side wall and the leading inner, leading midspan, leading outer, trailing inner, trailing midspan, and trailing outer surfaces.

Stationary Results

Before discussing the rotating results, it is necessary to discuss the stationary results. It is important to notice that, in the present test, the Reynolds number is controlled at 10,000, 20,000, 30,000, and 40,000 at the inlet of the test section. The local Reynolds number remaining in the channel is decreased due to the coolant flow ejected from the slots. The local Reynolds number distribution in the stationary channel is shown in Fig. 5. It shows that, when the inlet Reynolds number is 40,000, it decreases to about 6100 at the end of the channel, whereas when the inlet Reynolds number is 10,000, it decreases to about 1600 at the end of the channel.

In the nonrotating channel, the level of heat transfer is influenced by the channel shape. The coolant flow goes through a sudden contraction entrance and then enters the heated portion of the test section without being hydrodynamically developed. As the flow goes along the streamwise direction, it is discharged through the slot and the local mass flow rate decreases. The decrease in the coolant remaining in the channel leads to a decrease in the heat transfer

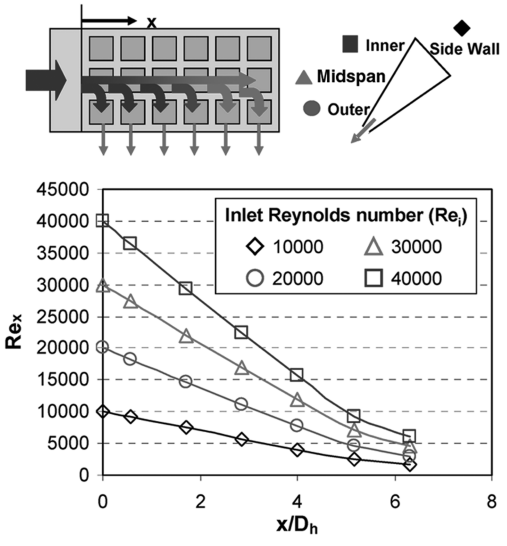

Fig. 5 Local Reynolds number distribution in the stationary channel.

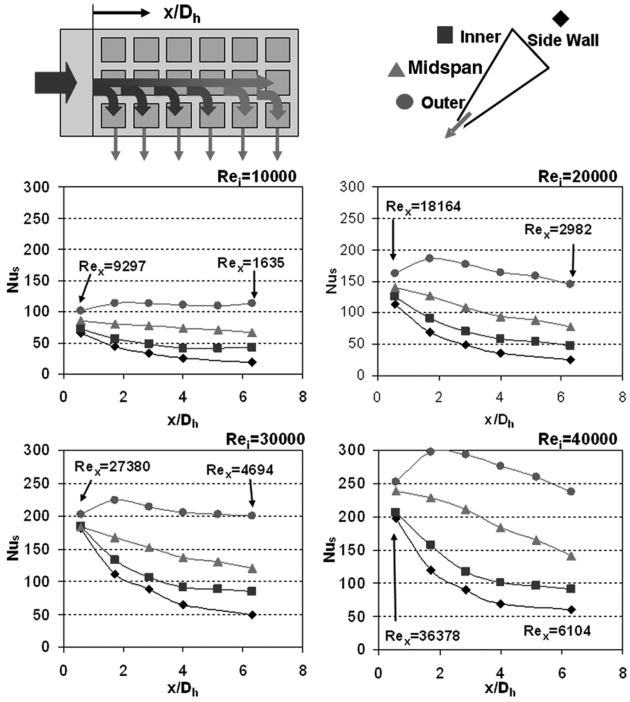

Fig. 6 Nusselt number distributions in the stationary channel.

coefficient along the streamwise direction. Figure 6 shows the Nusselt number distribution along the streamwise direction at four different inlet Reynolds numbers ($Re_i = 10,000$, 20,000, 30,000, and 40,000). The local Reynolds number (Re_x) at the first region ($x/D_h = 0.57$) and the last region ($x/D_h = 6.30$) is also labeled in the figure. As the inlet Reynolds number increases from 10,000 to 40,000, the Nusselt number also increases. On the outer surface, the flow turns 90 deg from the streamwise direction to the ejection slot, and this turning-induced secondary flow enhances the heat transfer. Furthermore, the slot ejection thins the boundary layer and strong turbulence mixing also occurs around this region. Therefore, heat transfer enhancement is the highest. In this region, the Nusselt number maintains the same level at the lowest Reynolds number case ($Re_i = 10,000$). However, the Nusselt number increases and then decreases for the other three Reynolds number cases.

The coolant flow tends to go toward the narrow region (outer surface) due to slot ejection, and the wide region (side wall and inner surface) has less coolant. Therefore, the heat transfer decreases from the narrow side toward the wide side, and the wide side (side wall) has the lowest heat transfer. For the side wall, the inner surface, and the midspan, the boundary layer is thicker than the outer surface due to less effect from the slot ejection. The Nusselt number decreases gradually along the streamwise direction due to the decrease in the local mass flow rate and the development of the boundary layer along the streamwise direction.

Rotating Results

It is necessary to discuss the general rotational behavior in the rotating channel before the discussion of the effect of rotation in the current cooling channel. For a rotating channel with radially outward flow, it has been well documented that the rotation-induced Coriolis force combines with the rotation-induced buoyancy force, so that heat transfer enhancement is observed in the trailing surface of the channel. This enhancement comes at the expense of reduced heat transfer coefficients on the leading surface [3–5]. Depending on how the channel is oriented (with respect to the direction of rotation) and the cross section of the channel, the rotation-induced secondary flow might be altered. In other words, studies have shown the most significant declination of the heat transfer coefficients on the leading surface occur in square channels rotating orthogonal to the direction of rotation [3]. However, if the channel is skewed at 135 deg with

respect to the direction of rotation, the heat transfer coefficients are enhanced on both the leading and trailing surfaces [10].

In the present study, the wedge-shaped channel with slot ejection is rotating with $\beta = 135$ deg. This specific geometry with slot ejection has many features that combine to profoundly affect the heat transfer coefficients within the channel. However, it is necessary to consider how rotation affects the heat transfer through the channel. Traditionally, conceptual descriptions of the rotation-induced secondary flow involve the formation of two counter-rotating vortices, as shown in Fig. 7. The vortices form in the cross section of the channel as the coolant is forced away from the leading surface to the trailing surface. As shown in Fig. 7, this behavior is likely to occur within the wide half (near the side wall and inner surface) of the channel. In other words, the coolant is forced away from the leading inner surface toward the trailing midspan and inner surfaces. In the very narrow region of the channel, these rotation-induced vortices begin to breakdown and no clear structure exists. Furthermore, strong turbulent mixing occurs at this region due to the slot ejection through the outer surface. The strong slot jet behavior tends to decrease toward the inner surface and side wall.

The local Reynolds number distribution is also measured under the rotating condition. The decreased Reynolds number produces a high rotation number, especially near the end of the channel. The local rotation number reaches about 7.5 at $x/D_h = 6.3$. Figure 8 is the test matrix showing the local rotation number distribution with respect to the local Reynolds number at three different streamwise locations for the current study.

To study the heat transfer enhancement (or declination) due to rotation, the ratio of rotating Nusselt number (Nu) to the stationary Nusselt number (Nu_s) distribution along the streamwise direction is plotted in Fig. 9. Four different Reynolds number cases, each at the highest rotational speed (500 rpm), are presented to show the effect of rotation. The Nu/Nu_s value on the trailing surface is higher than the leading surface for the inner, midspan, and outer surfaces. At the inner surface, the effect of rotation is strong and the difference of the Nu/Nu_s value between the leading and trailing surfaces is large. At the outer surface, the effect of rotation reduces and the difference between the leading and trailing surfaces is small. As the Reynolds number increases, the effect of rotation deceases.

The heat transfer enhancement is the highest at the trailing inner surface at $Re_i = 20,000$, 30,000, and 40,000.

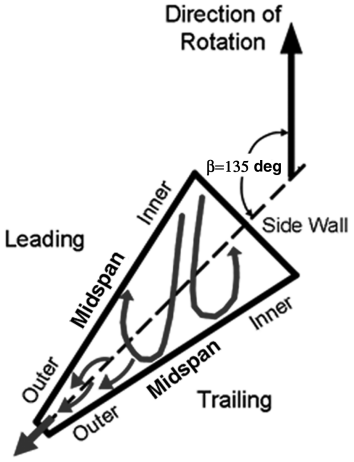

Fig. 7 Conceptual view of the rotation-induced secondary flow with slot ejection.

Rotation Number Effect

Rotation number is a relative measure of the rotational Coriolis force to the bulk flow inertia force (Han et al. [1]), which is a widely used nondimensional parameter in the industry and academia:

$$Ro = \Omega D_h / V \tag{6}$$

The flow velocity is based on the local mass flow rate measured at each region. To study the heat transfer enhancement, the ratio of measured Nusselt number (Nu) to the value from the fully developed flow (Nu_o) in a tube has been reported. The Nu_o is based on the local Reynolds number in each region. Figure 10 shows the Nu ratio (Nu/Nu_o) with respect to the local rotation number at three different locations. The Nusselt number did not follow the $Re^{0.8}$ relationship due to the effects of sharp entrance and channel geometry, and the slot ejection turning the flow. However, the Nu_o from the smooth tube is still chosen just for the heat transfer level comparison. The results presented here contain four different inlet Reynolds numbers with five different rotational speeds. We first look at the location of $x/D_h = 4.0$. Beginning with the side wall and inner surface, the effect of Reynolds number has been eliminated. On the trailing inner surface, the Nu ratio increases with the rotation number up to about 1.0 and then starts to decrease. For the inner surface and side wall, the heat transfer enhancement did not vary significantly. The trailing inner surface has higher Nu ratios than the leading inner surface and the side wall. On the outer surface, the Nu ratio increases with the

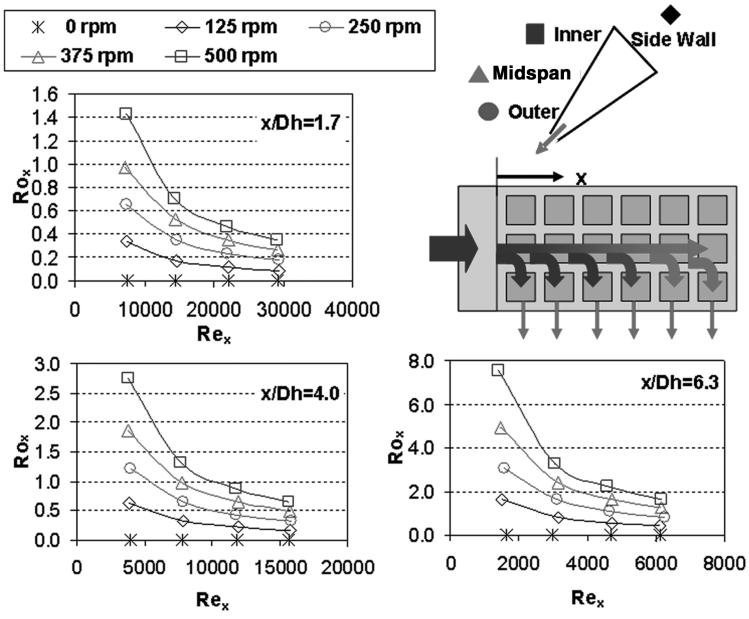

Fig. 8 Local rotation number (Ro_x) with respect to local Reynolds number (Re_x) at three different locations in the current test matrix.

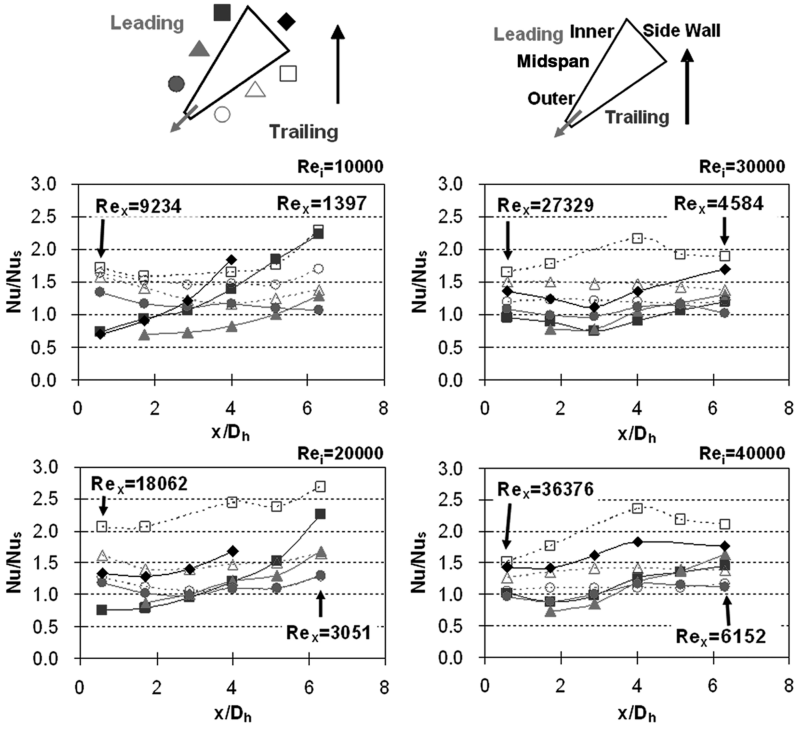

Fig. 9 Heat transfer enhancement (Nu/Nus) in the rotating channel (500 rpm).

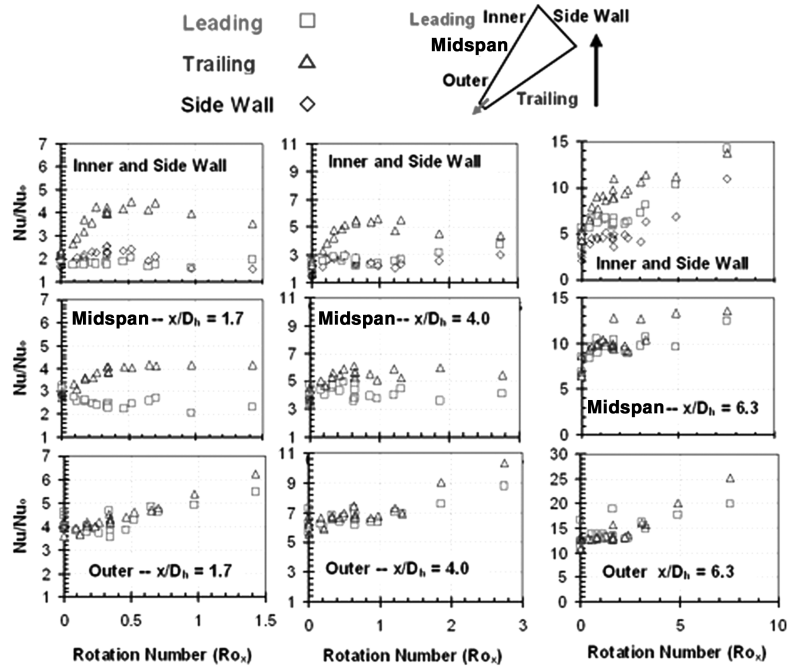

Fig. 10 Effect of rotation number on the Nusselt number ratios in the entrance, fully developed, and exit regions of the channel.

rotation number for both the leading and trailing surfaces. In the region near the entrance of the channel ($x/D_h = 1.7$), the trend is very similar to the $x/D_h = 4.0$ region. Near the end of the channel ($x/Dh = 6.3$), the trend is very similar in the midspan and outer surface. However, the heat transfer enhancement increases with the rotation number on both the leading inner and trailing inner surfaces and the side wall.

Although, as seen in the stationary results in Fig. 6, the heat transfer on the wide region is low. The heat transfer is enhanced on the trailing surface of the inner wall due to rotation. The side wall and the leading inner surface have similar heat transfer enhancement levels near the entrance of the channel. The coolant remaining in the channel is small downstream, and low heat transfer occurs in the stationary channel. However, the effect of rotation is strong due to low velocity and produces high heat transfer enhancement. At the downstream location of the channel ($x/D_h = 6.3$), the heat transfer is also enhanced, even on the wide region.

Buoyancy Parameter Effect

An additional way of presenting the Nusselt number ratio (Nu/Nu_o) is as a function of the local buoyancy parameter. As

shown in Eq. (7), the buoyancy parameter takes into the account the rotation-induced buoyancy force as well as the Coriolis force:

$$Bo_x = \left(\frac{\Delta\rho}{\rho}\right)_x Ro^2\left(\frac{R_x}{D_h}\right) = \left(\frac{T_{w,x} - T_{b,x}}{T_{f,x}}\right) Ro^2\left(\frac{R_x}{D_h}\right) \qquad (7)$$

A similar validation is needed for the buoyancy parameter that is needed for the rotation number: can the density ratio, rotation number, and rotating radius be varied independently, and with various combinations arrive at the same Nusselt number for the given buoyancy parameter? The local density ratio varies from approximately 0.05 to 0.11, and the local rotating radius varies from 61.5 to 74.2 cm. The local film temperature, $T_{f,x}$, is defined as the average of the local wall and coolant temperatures. Because of the temperature differences within the channel, the direction of the buoyancy force is away from the center of rotation. The strength of this force is determined by the density (or the temperature) difference in the fluid (from the heated wall to the cooler core). This nondimensional parameter is typically accepted as the preferred way to quantify the effect of rotation, as it includes all the parameters contributing to the effect of rotation. Figure 11 presents the Nusselt number ratios (Nu/Nu_o) plotted with the local buoyancy parameter. Similar trends shown in the plots with the rotation number can be observed in this figure. At the $x/D_h = 1.7$ location, the trailing surface has higher heat transfer enhancement than the leading surface on the inner surface and midspan. On the outer surface, the leading and trailing surfaces have similar Nusselt number ratios and both increase with the buoyancy parameter. At the $x/D_h = 4.0$ location, the difference between the leading and trailing surface becomes smaller in the midspan, whereas, as the flow moves further downstream, the coolant flow remaining in the channel decreases and the buoyancy parameter increases. The local buoyancy parameter is the highest in the $x/D_h = 6.3$ location.

Average Heat Transfer Results

The data has been presented for three specific locations within the channel. However, it is beneficial to observe the effect of rotation on the overall heat transfer enhancement. To begin this process, the Nusselt number ratios for each surface are averaged in the streamwise direction. Figure 12 shows these streamwise averages;

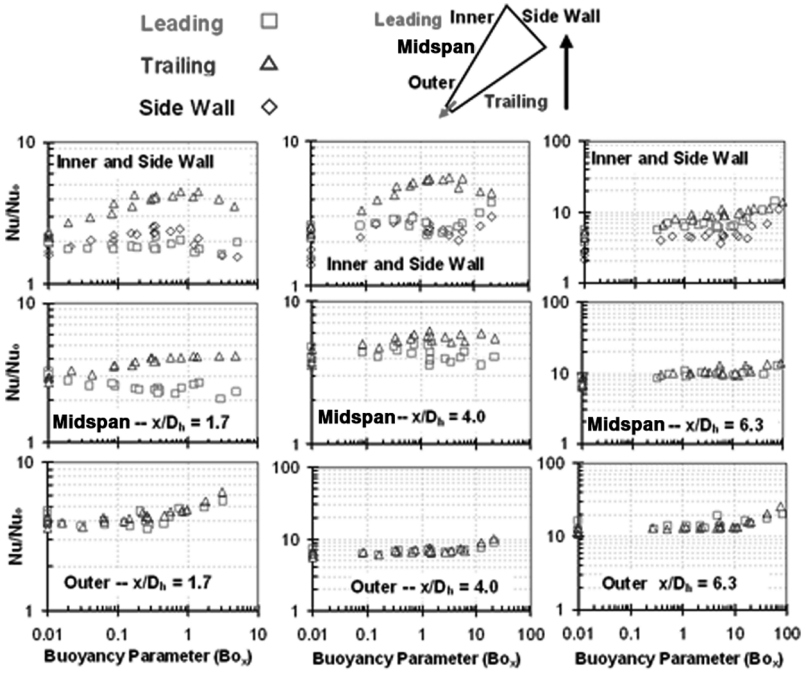

Fig. 11 Effect of buoyancy parameter on the Nusselt number ratios in the entrance, fully developed, and exit regions of the channel.

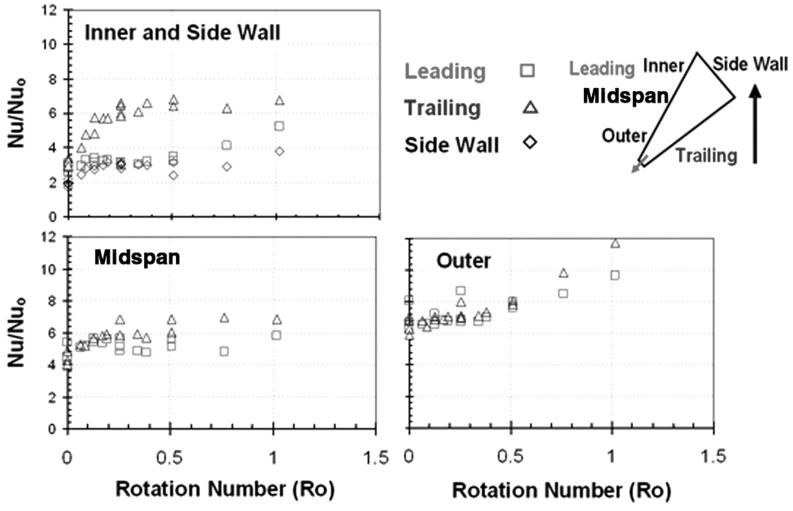

Fig. 12 Effect of rotation number on the streamwise averaged Nusselt number ratios.

each data represents the average of the six streamwise regions, plotted with the rotation numbers. The rotation number is also the average of the local rotation numbers in these six regions.

On the inner surface, the Nu ratio on the trailing surface increases with the rotation number until a critical rotation number of 0.5 is reached. The Nu ratio (Nu/Nu_o) reaches about 6.5, and the heat transfer enhancement is about 2 times higher compared with the stationary case.

The Nu ratio then maintains the same level when the rotation number is larger than 0.5. On the side wall and the leading inner surface, the Nu ratio does not vary significantly when the rotation number is smaller than 0.5. The Nu ratios in both regions begin to increase with the rotation number when the rotation number is larger than 0.5.

In the wide region of the channel, the effect of rotation is very obvious. The effect of rotation decreases toward the narrow side of the channel. The difference between the leading and trailing surface is smaller in the narrow region (midspan and outer) than the wide region (inner and side wall). The results on the midspan and outer surface are more scattered. On the outer surface, the Nu ratios on both the leading and trailing surfaces increase with the rotation number.

Figure 13 shows the streamwise averaged Nusselt number ratios with respect to the buoyancy parameter. The buoyancy parameters are also the average of the local buoyancy parameters of the six regions. Similar trends occur on the inner surface; the Nu ratio on the trailing surface increases with the buoyancy parameter until a critical buoyancy parameter of about 2.0 is reached and then maintains the same level when the buoyancy parameter is larger than 2.0. On the side wall and the leading inner surface, the Nu ratio remains the at same level when the buoyancy parameter is smaller than 6.0. The Nu ratios begin to increase with the buoyancy parameter when the buoyancy parameter is larger than 6.0. The results on the midspan and outer surface also show similar trends as plotted with the rotation number.

It has been established that the heat transfer enhancement varies across the entire channel. The average heat transfer enhancements on the leading and trailing surfaces are the results on the inner, midspan, and outer surfaces. The spanwise and streamwise averaged Nusselt number ratios are shown in Fig. 14. The coefficients for Eq. (8) are shown in Table 1. Each data point (on the leading and trailing surfaces) is now the average of the 18 points in that region. Over the range of Reynolds numbers and rotational speeds, each of the three surfaces follow very distinct trends, with the data for each surface collapsing to a common curve. Most notably, for all three surfaces, the Nusselt number ratios increase as the rotation number increases. The results are also presented with the averaged buoyancy

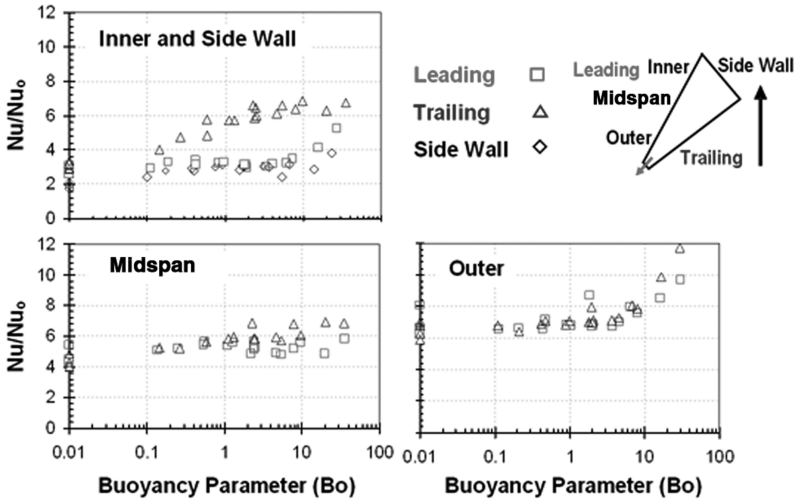

Fig. 13 Effect of buoyancy parameter on the streamwise averaged Nusselt number ratios.

	A	m	B	n
Leading	5	0.03	0.1	0.7
Trailing	5.5	0.02	0.3	0.6
Side wall	2.3	0.02	0.6	0.2

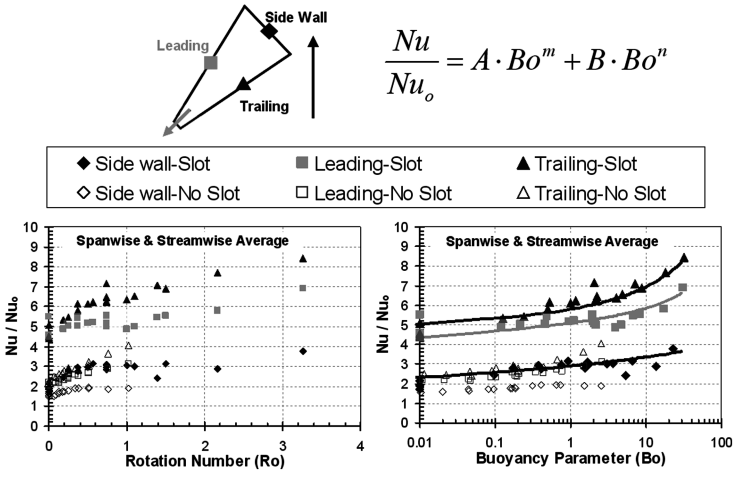

Fig. 14 Streamwise and spanwise averaged Nusselt number ratios with rotation number and buoyancy parameter.

Table 1 Coefficients for the correlation functions in Fig. 14

	A	m	B	n
Leading	5	0.03	0.1	0.7
Trailing	5.5	0.02	0.3	0.6
Side wall	2.3	0.02	0.6	0.2

parameters. The results of the smooth wedge-shaped channel without slot ejection from Wright et al. [26] are also plotted as a comparison with the current study. The heat transfer enhancement is much higher than the cases without slot ejection. The correlations have been generated as a function of the buoyancy parameter:

$$Nu/Nu_o = A \cdot Bo^m + B \cdot Bo^n \tag{8}$$

Wright et al. [26] already proved that the data in a smooth wedge-shaped channel can be correlated as a function of the buoyancy parameter. When the effect of slot ejection is considered in the wedge-shaped channel, it still shows that the data can be correlated with the buoyancy parameter from the combination of variable Reynolds numbers and rotational speeds.

Conclusions

This paper investigated the wedge-shaped cooling channel with slot ejection applicable to the trailing edge of the turbine blade. Regionally averaged heat transfer coefficients are measured in the streamwise and spanwise directions. The amount of coolant flow extracted from each slot is measured to determine the coolant remaining in the channel. All the tests were performed at four different inlet Reynolds numbers (10,000–40,000) with five different rotational speeds (0–500 rpm). The effect of rotation affected by the high rotation number and high buoyancy parameter was tested to satisfy the real engine condition. Based on the results reported, the following conclusions can be drawn:

1) Based on the results from the stationary channel, due to the slot ejection in the narrow region of the channel, the Nusselt number is the highest in this region, whereas the lowest Nusselt number occurs in the wide region of the channel. However, when the effect of rotation is considered, it also enhances heat transfer in the wide region.

2) The slot ejection creates turbulent mixing around the narrow region, and the effect of rotation is smaller in the narrow region than the wide region of the wedge-shaped channel.

3) Because of the radially outward flow and the channel orientation of 135 deg, the heat transfer on both the leading and trailing surfaces are enhanced with rotation. Higher heat transfer enhancement occurs on the trailing surface than the leading surface. Critical rotation number and buoyancy parameters still exist where the trend of the heat transfer enhancement begins to change.

4) The average heat transfer enhancement with the slot ejection case is higher than the no-slot case.

5) The rotation number and buoyancy parameter are still good parameters to quantify the effect of rotation with the slot ejection in the wedge-shaped cooling channel. Both of them can be applied locally (based on the local mass flow rate) or the average value over the entire surface.

Acknowledgment

This work has been funded through the Marcus Easterling Endowment fund.

References

[1] Han, J. C., Dutta, S., and Ekkad, S. V., *Gas Turbine Heat Transfer And Cooling Technology*, Taylor And Francis, New York, 2000.

[2] Kays, W. M., and Crawford, M. E., *Convective Heat and Mass Transfer*, 3rd ed., McGraw–Hill, New York, 1993, pp. 311–349.

[3] Wagner, J. H., Johnson, B. V., and Hajek, T. J., "Heat Transfer in Rotating Passage with Smooth Walls and Radial Outward Flow," *Journal of Turbomachinery*, Vol. 113, No. 1, 1991, pp. 42–51. doi:10.1115/1.2927736

[4] Wagner, J. H., Johnson, B. V., and Kopper, F. C., "Heat Transfer in Rotating Passage with Smooth Walls," *Journal of Turbomachinery*, Vol. 113, No. 3, 1991, pp. 321–330. doi:10.1115/1.2927879

[5] Johnson, B. V., Wagner, J. H., Steuber, G. D., and Yeh, F. C., "Heat Transfer in Rotating Serpentine Passage with Selected Model Orientations for Smooth or Skewed Trip Walls," *Journal of Turbomachinery*, Vol. 116, No. 4, 1994, pp. 738–744. doi:10.1115/1.2929467

[6] Dutta, S., and Han, J. C., "Local Heat Transfer in Rotating Smooth and Ribbed Two-Pass Square Channels with Three Channel Orientations," *Journal of Heat Transfer*, Vol. 118, No. 3, 1996, pp. 578–584. doi:10.1115/1.2822671

[7] Park, C. W., and Lau, S. C., "Effect of Channel Orientation of Local Heat (Mass) Distributions in a Rotating Two-Pass Square Channel with Smooth Walls," *Journal of Heat Transfer*, Vol. 120, No. 3, 1998, pp. 624–632. doi:10.1115/1.2824323

[8] Bons, J. P., and Kerrebrock, J. L., "Complementary Velocity and Heat Transfer Measurements in a Rotating Cooling Passage with Smooth Walls," *Journal of Turbomachinery*, Vol. 121, No. 4, Oct. 1999, pp. 651–662.

[9] Azad, G. S., Uddin, M. J., Han, J. C., Moon, H. K., and Glezer, B., "Heat Transfer in a Two-Pass Rectangular Rotating Channel with 45-Deg Angled Rib Turbulators," *Journal of Turbomachinery*, Vol. 124, No. 2, 2002, pp. 251–259. doi:10.1115/1.1450569

[10] Griffith, T. S., Al-Hadhrami, L., and Han, J. C., "Heat Transfer in Rotating Rectangular Cooling Channels ($AR = 4$) with Angled Ribs," *Journal of Heat Transfer*, Vol. 124, No. 4, 2002, pp. 617–625. doi:10.1115/1.1471525

[11] Wright, L. M., Lee, E., and Han, J. C., "Influence of Entrance Geometry on Heat Transfer in Rotating Rectangular Cooling Channels (AR = 4:1) with Angled Ribs," *Journal of Heat Transfer*, Vol. 127, No. 4, 2005, pp. 378–387. doi:10.1115/1.1860564

[12] Acharya, S., Agarwal, P., and Nikitopoulos, D. E., "Heat/Mass Transfer in a 4:1 AR Smooth and Ribbed Coolant Passage with Rotation in 90-Degreee and 45-Degree Orientations," American Society of Mechanical Engineers Paper GT2004-53928, June 2004.

[13] Zhou, F., Lagrone, J., and Acharya, S., "Internal Cooling in 4:1 AR Passages at High Rotation Numbers," American Society of Mechanical Engineers Paper GT2004-53501, June 2004.

[14] Fu, W. L., Wright, L. M., and Han, J. C., "Heat Transfer in Two-Pass Rotating Rectangular Channels (AR = 1:2 and AR = 1:4) with Smooth Walls," *Journal of Heat Transfer*, Vol. 127, No. 3, 2005, pp. 265–277. doi:10.1115/1.1857946

[15] Fu, W. L., Wright, L. M., and Han, J. C., "Buoyancy Effects on Heat Transfer in Five Different Aspect-Ratio Rectangular Channels with Smooth Walls and 45-Degree Ribbed Walls," American Society of Mechanical Engineers Paper GT 2005-68493, May 2005.

[16] Lowdermilk, W. H., Weiland, W. F., and Livingood, J. N. B., "Measurement of Heat Transfer and Friction Coefficients for Flow of Air in Noncircular Ducts at High Surface Temperatures," NACA RM E53J07, 1954.

[17] Ahn, S. W., and Son, K. P., "Heat Transfer and Pressure Drop in the Roughened Equilateral Triangular Duct," *International Communications in Heat and Mass Transfer*, Vol. 29, No. 4, 2002, pp. 479–488. doi:10.1016/S0735-1933(02)00345-7

[18] Obot, N. T., "Heat Transfer in a Smooth Scalene Triangular Duct with Two Rounded Corners," *International Communications in Heat and Mass Transfer*, Vol. 12, No. 3, 1985, 1pp. 251–258. doi:10.1016/0735-1933(85)90048-X

[19] Zhang, Y. M., Gu, W. Z., and Han, J. C., "Augmented Heat Transfer in Triangular Ducts with Full and Partial Ribbed Walls," *Journal of Thermophysics and Heat Transfer*, Vol. 8, No. 3, 1994, pp. 574–579. doi:10.2514/3.580

[20] Harasgama, S. P., and Morris, W. D., "The Influence of Rotation on the Heat Transfer Characteristic of Circular, Triangular, and Square-Sectioned Coolant Passages of Gas Turbine Rotor Blades," *Journal of Turbomachinery*, Vol. 110, No. 1, 1988, pp. 44–50.

[21] Dutta, S., Han, J. C., and Lee, C. P., "Local Heat Transfer in a Rotating Two-Pass Ribbed Triangular Duct with Two Model Orientations,"

International Journal of Heat and Mass Transfer, Vol. 39, No. 4, 1996, pp. 707–715.
doi:10.1016/0017-9310(95)00171-9

[22] Kumaran, T. K., Han, J. C., and Lau, S. C., "Augmented Heat Transfer in a Pin Fin Channel with Short or Long Ejection Holes," *International Journal of Heat and Mass Transfer*, Vol. 34, No. 10, 1991, pp. 2617–2628.
doi:10.1016/0017-9310(91)90101-J

[23] Taslim, M. E., Li, T., and Spring, S. D., "Experimental Study of the Effects of Bleed Holes on Heat Transfer and Pressure Drop in Trapezoidal Passages with Tapered Turbulators," *Journal of Turbomachinery*, Vol. 117, No. 2, 1995, pp. 281–289.

[24] Hwang, J. J., and Lu, C. C., "Lateral-Flow Effect on Endwall Heat Transfer and Pressure Drop in a Pin Fin Trapezoidal Duct with Various Pin Shapes," *Journal of Turbomachinery*, Vol. 123, No. 1, 2001, pp. 133–139.
doi:10.1115/1.1333093

[25] Liu, Y. H., Huh, M., Han, J. C., and Chopra, S., "Heat Transfer in a Two-Pass Rectangular Channel (AR = 1:4) Under High Rotation Numbers," American Society of Mechanical Engineers Paper GT 2007-27067, May 2007.

[26] Wright, L. M., Liu, Y. H., Han, J. C., and Chopra, S., "Heat Transfer in Trailing Edge, Wedge-Shaped Cooling Channels Under High Rotation Numbers," American Society of Mechanical Engineers Paper GT 2007-27093, May 2007.

[27] Kline, S. J., and McClintock, F. A., "Describing Uncertainty in Single-Sample Experiments," *Mechanical Engineering*, Vol. 75, No. 1, 1953, pp. 3–8.